Atmospheric Environment 42 (2008) 6749–6758

Contents lists available at ScienceDirect

Atmospheric Environment

journal homepage: www.elsevier.com/locate/atmosenv

The morphology of ultrafine particles on and near major freeways

Teresa L. Barone [a], Yifang Zhu [b,*]

[a] Oak Ridge National Laboratory, Oak Ridge, TN 37831, USA
[b] Department of Environmental Engineering, Texas A&M University – Kingsville, 700 University Boulevard, MSC 213, Kingsville, TX 78363, USA

ARTICLE INFO

Article history:
Received 10 December 2007
Received in revised form 20 May 2008
Accepted 21 May 2008

Keywords:
Ultrafine particles
Morphology
Particulate matter
Size distribution
Vehicular emissions
Near roadway environment

ABSTRACT

The morphology of ultrafine particles (UFPs; diameter < 100 nm) collected on and near major Los Angeles freeways in April 2006 is reported. Samples were size selected with a differential mobility analyzer, collected by a nanometer aerosol sampler, and analyzed using a transmission electron microscope. Typical observed morphologies included aggregates, spheres, irregularly shaped particles, and particles with multiple inclusions. For freeway aerosols with 50 nm electrical mobility diameter, most (>90%) electron-opaque particles were surrounded by an electron-transparent material. This suggests that much of these particles were heterogeneously internally mixed. The fraction of UFPs in a given morphology class collected on and at increasing downwind distance from the I-405 freeway was compared. The fraction of aggregates measured 90 m downwind of I-405 was significantly less than the fraction measured on the freeway (p-value < 0.01). Because aggregates are a primary aerosol (directly emitted), this may indicate that secondary aerosol (formed in the atmosphere) becomes more prevalent with increasing distance from the freeway. The fraction of particles with multiple inclusions measured 90 m downwind of I-405 was significantly greater than the fraction measured on the freeway (p-value < 0.01). The increase in the number of particles with multiple inclusions with increasing distance from the freeway suggests that dilution does not prevent particles from colliding and merging which may alter the particle size distribution.

1. Introduction

Particle morphology influences particle optical properties in the atmosphere (Bond and Bergstrom, 2006) and may affect how particles interact with lung epithelial cells (Stearns et al., 2001). Whether ultrafine particles (UFPs; diameter < 100 nm) are present as single spheres or aggregated spheres affects their deposition efficiency in the lung (Oberdörster, 2001). The morphology of atmospheric aerosols has been found to differ with respect to particle size range, location of sampling, and collection method. Typical reported morphologies included aggregates, spheres, irregularly shaped, and bar-shaped particles (Katrinak et al., 1993; Dye et al., 2000; Xiong and Friedlander, 2001; Okada and Heintzenberg, 2003; Shi et al., 2003; Yue et al., 2006). In addition, volatile particles with non-volatile inclusions have been observed using a transmission electron microscope (TEM) (Okada and Heintzenberg, 2003). Atmospheric particle volatility was associated with the electron-opacity of the particle after bombardment with the electron beam in the TEM.

Diesel and gasoline vehicle emissions are major sources of UFPs in urban environments and usually consist of solid soot aggregates coated with an adsorbed hydrocarbon and sulfate layer, volatile organic and sulfuric acid droplets, and ash (Kittelson, 1998). Wentzel et al. (2003) measured an average primary particle diameter of 22.6 ± 6 nm and fractal dimension of 1.70 ± 0.13 for diesel aggregates using TEM analysis. For aggregates emitted by a spark-ignition (SI) engine, Chakrabarty et al. (2006) observed a bimodal primary particle size distribution (20–24 nm and 54–60 nm) during a driving cycle which incorporated high

* Corresponding author. Tel.: +1 361 593 3898; fax: +1 361 593 2069.
E-mail address: yifang.zhu@tamuk.edu (Y. Zhu).

1352-2310/$ – see front matter © 2008 Elsevier Ltd. All rights reserved.
doi:10.1016/j.atmosenv.2008.05.019

vehicle speeds. The fractal dimension of SI engine-emitted aggregates ranged from 1.7 to 1.78. Mathis et al. (2004) analyzed volatile diesel and SI engine exhaust particles by TEM and found that particles in the size range of about 10–40 nm were generally spherical. They grouped these particles into three classes: a highly volatile hydrophilic group, a less volatile hydrophobic group, and a mixture of both, which had intermediate volatility. Rönkkö et al. (2007) observed an abundance of volatile UFPs with a non-volatile core emitted from a heavy-duty diesel engine equipped with exhaust gas recirculation. Their results were based on the comparison of particle number–size distributions for exhaust with and without treatment of a thermodenuder. Khun et al. (2005) assessed the volatility of UFPs near a light-duty vehicle freeway using a tandem differential mobility analyzer (TDMA) with a heater between the two DMAs. Their measurements indicate that a large fraction of near-freeway UFPs consists of volatile material. It was observed that 94% of 40 nm and 80% of 80 nm particles were internally mixed. For particles larger than the ultrafine size range, irregularly shaped ash was present in diesel exhaust (Bérubé et al., 1999) and emissions from combusting fuel oil in a three-pass fire-tube package boiler (Chen et al., 2004).

UFPs make up most of the total atmospheric particle number concentrations, and are present at concentrations of about 10^4 particles cm^{-3} of air in Southern California cities (Cass et al., 2000). Higher total particle number concentrations are present near major freeways than in community air in Los Angeles, CA (Zhu et al., 2002a,b; Zhu et al., 2004). For particles in different size ranges, distinct number concentration decay characteristics were found with distance from freeways (Zhu et al., 2002a). The data suggested coagulation had occurred. However, in a later multi-component sectional aerosol dynamic model analysis of the same data set, Zhang et al. (2004) found that changes in the number–size distribution occurred mainly due to condensation and evaporation processes, and that coagulation and deposition had little effect. Morphological analysis of UFPs with distance from a freeway may give insight on the processes involved in altering the number–size distribution. For example, an increase in the number of solid particles with a liquid film may be evidence of particle growth by condensation.

The change in atmospheric particle morphology with increasing distance from a roadside has not been examined previously. Only one study has characterized the morphology of atmospheric particles near a roadway (Dye et al., 2000) in which a higher fraction of aggregates was measured in roadside aerosol (94%) than in urban background aerosol (89%). It was suggested that this was due to condensation and evaporation on the particle surface, agglomeration, and coating that caused the aggregates to restructure to compact solid particles during aerosol transport from roadside to community air. However, atmospheric aggregates were not found to become more compact following condensation and evaporation of water on their surface (Kim et al., 2001). This discrepancy illustrates that the mechanisms which alter the morphology of atmospheric aerosol as it moves from the roadside to community air are not fully understood.

In this paper, we report typical UFP morphologies observed on and near two major Los Angeles freeways. The number fraction of UFPs of a given morphology on a freeway and 30, 60, and 90 m downwind of the freeway was compared. To our knowledge, this is the first study to measure changes in atmospheric UFP morphology with increasing distance from a freeway.

2. Methods

2.1. Sampling sites and measurement periods

Measurements were made using a mobile laboratory developed for on-freeway particulate matter exposure health studies (Zhu et al., 2008). Samples were collected while driving on two Los Angeles freeways (i.e., I-405 and I-710) with distinct fractions of heavy-duty diesel trucks on April 21 and 25, 2006. Samples were also collected 30, 60, and 90 m downwind of I-405 on Constitution Avenue on April 24, 28, and 29, 2006.

UFPs were sampled for 1 h at each distance for near-freeway measurements and 30 min for on-freeway measurements. Meteorological conditions and traffic density were similar for I-405 on- and near-freeway measurements. This is important, because it allows samples from different days to be aggregated together. The mean and standard deviation of wind speed, temperature, relative humidity, barometric pressure, and total particle number (#) concentration were 6.3 ± 1.2 mph, 64.4 ± 1.5 F, $61.7 \pm 8.1\%$, 29.67 ± 0.75 in Hg, and $(5.25 \pm 1.29) \times 10^4$ # cm^{-3}, respectively. During the near-freeway sampling period (10 am–2 pm), a consistent sea breeze (parallel to Constitution Ave.) developed and brought freeway aerosols to the sampling sites. No significant UFP sources were observed upwind of the freeway near the sampling points. A detailed description of the I-405 sampling site can be found in Zhu et al. (2002a). I-405 and I-710 on-freeway measurements were made on days in which the temperature, relative humidity and barometric pressure were fairly similar; their mean and standard deviation were 62.8 ± 1.7 F, $63.2 \pm 7.1\%$, and 29.20 ± 0.94 in Hg, respectively. However, the wind speed was about 40% less and the total particle concentration 60% greater on I-710 than on I-405. These differences are discussed in Section 3.4.

2.2. Instrumentation

Freeway aerosols were charged by a bipolar diffusion charger and size selected for 50 nm particles using a differential mobility analyzer (DMA, Model 3080, TSI Inc., Shoreview, MN). The electrical mobility diameter (d_e) 50 nm was selected because it was in the second mode of the number–size distribution for aerosol near I-405, which allows the observation of the change in prominence from the smaller to the larger modes (Zhu et al., 2002a). The sample and sheath flow rates were 2 and 20 L min^{-1}, respectively. The size-selected aerosol was passed through a nano-aerosol sampler (NAS, Model 3089, TSI Inc., Shoreview, MN), which had an electric potential of 10 kV. Particles were deposited on a TEM grid that was fixed to the electrode in the NAS. The NAS is an electrostatic

precipitator, which was designed to collect charged nanoparticles on a substrate for off-line analysis. In a conventional electrostatic precipitator, particle charging and collection takes place simultaneously. In this alternative design, the aerosol is charged before entering the NAS for collection. The NAS was chosen for sample collection for the following reasons: (1) it was designed such that particles are collected uniformly on the sample substrate. Thus, a small fraction of the sample could be analyzed that is representative of the whole. (2) It has less power requirements than an impactor, so it could be used in conjunction with a battery supply on a mobile laboratory unit for on-freeway measurements. (3) Particles in the nanometer size range are collected with high efficiency.

The total (non-size selected) on- and near-freeway aerosols were also sampled. The total aerosol was charged by the bipolar diffusion charger and passed through the NAS at 1 L min^{-1} and 10 kV for collection. For each experimental condition, one sample was collected on a 400-mesh copper TEM grid with a carbon/formvar film (Electron Microscopy Sciences, PA). The formvar component provided extra support to prevent fracture of the film during sampling. For each experimental condition, ~500 particles were randomly selected out of ~10,000 particles collected. In total, about 2500 particles were individually analyzed for the five studied conditions, i.e., on I-405, on I-710, 30, 60, and 90 m downwind of I-405. Samples were analyzed using a JEOL 100 CX TEM (JEOL, Tokyo, Japan) at magnifications of 2×10^4 to 10^5.

Particle number–size distributions, in the 6–220 nm diameter range, were measured using a scanning mobility particle sizer (SMPS 3936L85, TSI Inc., St. Paul, MN). The SMPS consisted of a DMA (Model 3080) and a water condensation particle counter (WCPC; Model 3781, TSI Inc., Shorview, MN). Size distributions were measured at 2 min intervals by the SMPS continuously during sample collection with the DMA and NAS. SMPS output was exported in the Aerosol Instrument Manager software (version 5.1, TSI Inc., St. Paul, MN).

2.3. Uniformity of particle deposition in NAS

The uniformity of particle deposition on the sample substrate was examined. It is important for the particles to be uniformly distributed so that a small part of the substrate can be analyzed that is representative of the whole. The TEM grid is a copper lattice coated with a carbon/formvar film. Particles are observed on the transparent squares (mesh; 37×37 μm) of the grid. The number of particles per mesh was determined for one of the sampling conditions used in the experiment. We found the standard deviation in the number of particles per mesh was less than 10% indicating fairly uniform deposition. Thus, only about 5% of the particles, approximately 500 were randomly selected for TEM analysis under each experimental condition.

2.4. UFP collection efficiency by the NAS

NAS collection efficiency is discussed (in what follows) to examine whether particles of a given morphology are preferentially collected. Preferential collection of a given morphology is detrimental, because it would inhibit an unbiased comparison. In addition, collection efficiency is discussed to show that the fraction of particles of given morphology can be compared at varying distance from the freeway, but the results cannot be used to calculate the actual fraction present in the near-freeway aerosol.

The collection efficiency of the NAS depends on the particle electrical mobility diameter, and was determined previously by the manufacturer for spherical particles at 1 L min^{-1} and 10 kV setting (TSI Inc., 2001). Under this condition, particles with 50 nm d_e (the size selected for our study) are expected to be collected with greater than 90% efficiency. Since the flow rate of our study (2 L min^{-1}) was larger than 1 L min^{-1}, the collection efficiency was probably less than 90%. This is because at a higher flow rate, the residence time of the particles in the region near the electrode decreases, so there is less time for electrical migration. Since the collection efficiency was not measured previously for the flow rate of our study and for aggregates, the fraction of particles collected cannot be related to the fraction of particles present in the atmosphere. However, the change in the fraction of particles collected with respect to increasing distance from the freeway can be compared.

The performance of a device with similar geometry as the NAS was modeled previously by solving numerically the steady-state Navier–Stokes equation for incompressible flow, the convective-diffusive aerosol transport equation with electrostatic and gravitational external forces, and the Laplace equation for the electrical potential (Dixkens and Fissan, 1999). The model results indicate that the major mechanism of particle collection is electrostatic precipitation, by which particles of a given electrical mobility migrate and deposit on an oppositely charged surface. Diffusion played a minor role in the collection of particles larger than 10 nm, and contributed less than 1% to the collection efficiency of 50 nm particles. However, this model did not account for the dependence of the drag force on particle morphology which may be a source of error in their analysis.

In what follows, we consider whether a sphere and an aggregate may deposit differentially by diffusion. Differential deposition by diffusion is undesirable because it would result in the disproportionate collection of particles of a given morphology and a bias in the fraction measured. Before collection, particles of a given electrical mobility diameter are selected. An aggregate and a sphere with unit charge and the same electrical mobility diameter have the same migration velocity (Lall and Friedlander, 2006). Particle migration velocity (c_e) is given by the following expression (Friedlander, 2000):

$$c_e = \frac{ieE}{f} \tag{1}$$

where i is the number of charges, e is the electronic charge, E is the electric field intensity, and f is the friction coefficient. Thus, a sphere and an aggregate with unit charge in the presence of the same electric field, have the same friction coefficient. The diffusion coefficient (D) depends on the friction coefficient as described by the Stokes–Einstein equation (Friedlander, 2000):

$$D = \frac{kT}{f} \quad (2)$$

where k is the Boltzmann constant and T is the temperature. If the friction coefficient of a sphere and an aggregate with unit charge are the same, the diffusion coefficients would be equivalent. Thus, because the aerosol has been size selected for a given electrical mobility diameter, the diffusion coefficient of a sphere and an aggregate are expected to be the same. This implies that spheres and aggregates may not be differentially collected in the NAS.

The above analysis was carried out assuming that spheres and aggregates both have single charge, but their charging efficiency may differ (Lall and Friedlander, 2006). In the bipolar diffusion charger of the DMA for 50 nm d_e, the charging efficiency of singly charged aggregates (20–30 nm primary particle diameter) can be 10–20% greater than that for singly charged spheres (Lall and Friedlander, 2006). Because aggregates have a greater charging efficiency, they would be preferentially collected. For this reason, we do not compare the fraction of spheres and aggregates sampled. However, we compare of the change in fraction of a given morphology at increasing distances from the freeway.

We also evaluated whether a significant portion of particles would be deposited in the NAS by inertial impaction. The impaction parameter (Stokes number) was evaluated for a sphere (Stk_{sph}) and an idealized aggregate (Stk_{agg}) (Lall and Friedlander, 2006) with 50 nm electrical mobility diameter for the entrance conditions. For a sphere, the Stokes number is given by the following expression (Hinds, 1999):

$$Stk_{sph} = \frac{\rho_0 d_p^2 U_j C(d_p)}{18\mu L_j} \quad (3)$$

where ρ_0 is unit density, d_p is the particle diameter, U_j is the jet velocity, L_j is the jet diameter, $C(d_p)$ is the slip correction factor, and μ is the air viscosity. As derived in Barone et al. (2006), the following expression can be utilized for the Stokes number of an ultrafine aggregate:

$$Stk_{agg} = \frac{\lambda\pi\rho_p d_{pp} U_j}{3c^* \mu L_j} \quad (4)$$

where λ is the mean free path of the gas ($\sim$65 nm at atmospheric pressure), ρ_p is the primary particle density (1.77 gcm^{-3} for diesel aggregates measured by Park et al. (2004a)), d_{pp} is the primary particle diameter, and c^* is the dimensionless drag force which depends on aggregate orientation in the flow (Chan and Dahneke, 1981). Eq. (4) applies to idealized aggregates in the free molecular regime, for which the value of the Knudsen number ($Kn = 2\lambda/d_{pp}$) ≥ 10 (Lall and Friedlander, 2006). In this study, aggregates had a d_{pp} of approximately 20 nm and the value of Kn was about 6. Although the Kn value is less than 10, Eq. (4) was used to obtain an approximate estimate.

Because Stk_{agg} is a function of c^*, it depends on aggregate orientation in the flow. Previous experimental observations indicate that particles with large length to width ratios align with major axis parallel to the flow in an inertial impactor operated at near atmospheric pressure (Kasper and Shaw, 1983; Morigi et al., 1999). Thus, 6.62 was used for c^* for parallel orientation in the calculation of Stk_{agg} (Dahneke, 1982).

The values of Stk_{sph} and Stk_{agg} were evaluated for the sample flow rate 2 L min^{-1}, which corresponds to an entrance velocity 265 cm s^{-1}. Stk_{sph} and Stk_{agg} are 0.54×10^{-5} and 1.6×10^{-5}, respectively. Because the values are <1, it is expected that inertial impaction plays a minor role (Hinds, 1999).

3. Results and discussion

3.1. Typical UFP morphologies on- and near-freeway

Typical UFP morphologies collected on- and near-freeway are shown in Fig. 1. Because our sampling technique, sampling location, and particle size range differed from previous atmospheric particle morphology studies, a direct comparison of the types of morphologies collected cannot be made. However, similarities are mentioned below to provide some frame of reference. Consistent with previous studies, spheres (Dye et al., 2000; Xiong and Friedlander, 2001; Okada and Heintzenberg, 2003; Yue et al., 2006), aggregates (Katrinak et al., 1993; Dye et al., 2000; Xiong and Friedlander, 2001; Okada and Heintzenberg, 2003; Shi et al., 2003; Yue et al., 2006) and irregularly shaped particles (Dye et al., 2000; Okada and Heintzenberg, 2003; Yue et al., 2006) were present in our samples. In addition, particles with inclusions were observed as in the study of Okada and Heintzenberg (2003). Furthermore, the presence of aggregates and spheres is consistent with morphology studies of vehicle-emitted particles (Wentzel et al., 2003; Mathis et al., 2004; Chakrabarty et al., 2006). Adopting the terminology of Okada and Heintzenberg (2003), particles are denoted as electron-opaque and electron-transparent as a qualitative description of differing materials which compose particles observed by TEM. Thus, we grouped the aerosol into the following morphology classes: aggregates (Fig. 1a), electron-opaque spheres (Fig. 1b), electron-transparent spheres (Fig. 1c), irregularly shaped particles (Fig. 1d), and particles with multiple inclusions (Fig. 1e).

Chemical analysis of individual particles by energy dispersive X-ray spectrometry or electron energy loss spectroscopy was not feasible during the period of this study. It is intended to pursue this important aspect in a future study. For on- and near-freeway samples, UFP aggregates are most likely carbonaceous by-products of gasoline and diesel combustion. Electron-opaque spheres (Fig. 1b) may be solid or consist of a liquid with low volatility which did not evaporate in the low pressure environment of the TEM. Electron-transparent spheres (Fig. 1c) may be the thin film left behind after the evaporation of volatile organic carbon and/or sulfuric acid droplets (Okada and Heintzenberg, 2003; Mathis et al., 2004). Irregularly shaped particles were electron-opaque and may be solid or consist of a low volatility liquid (Fig. 1d). Metallic irregularly shaped particles are present in diesel exhaust, but their size is in the super micron range (Bérubé et al., 1999; Chen et al., 2004). Thus, it is more likely that ultrafine irregularly shaped particles are carbonaceous. A single

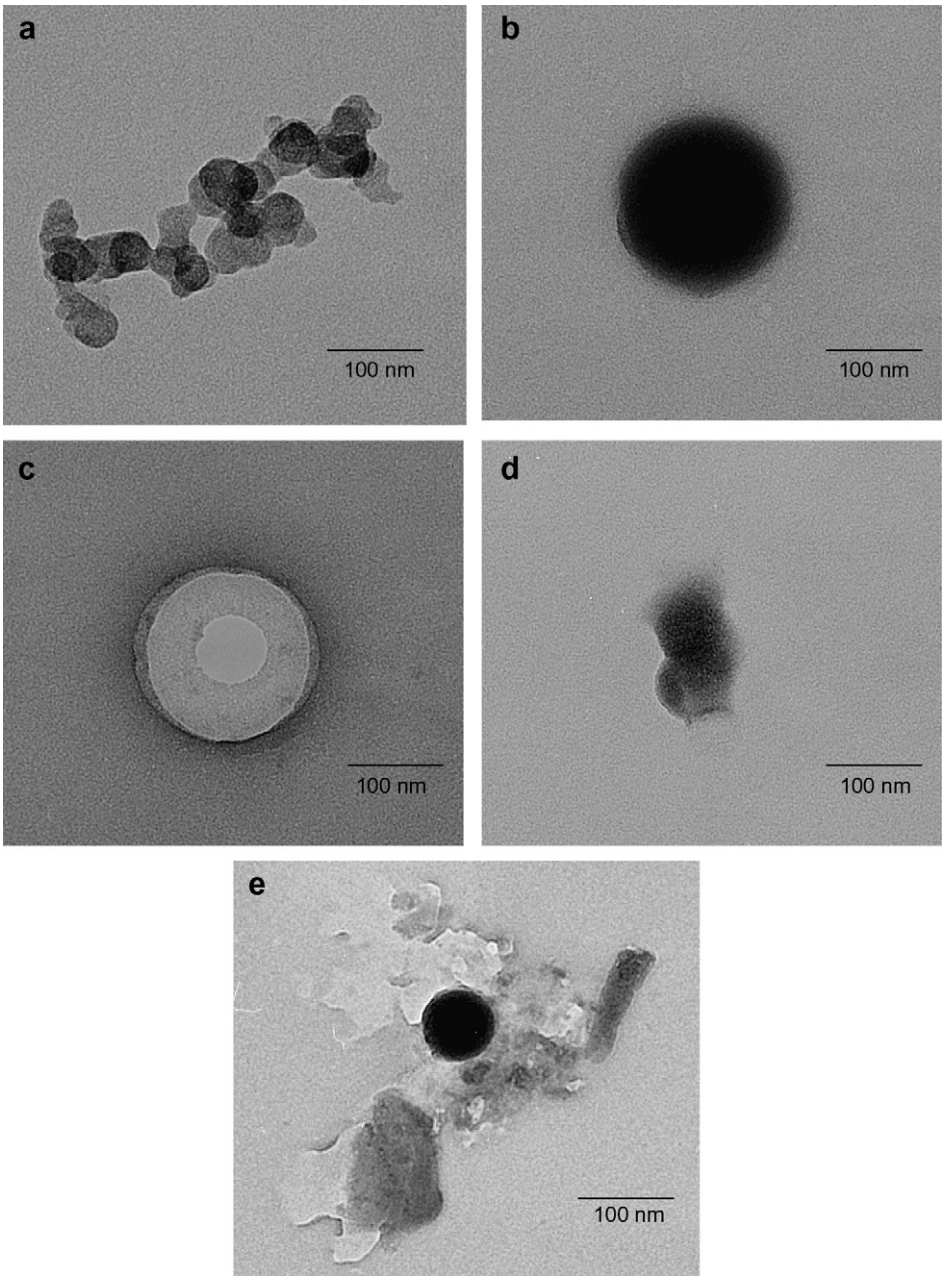

Fig. 1. TEM photomicrograph of (a) an aggregate, (b) electron-opaque sphere, (c) electron-transparent sphere, (d) irregularly shaped particle and (e) particle with multiple inclusions collected on- and near-I-405 by the NAS.

liquid particle with multiple inclusions (Fig. 1e) was electron-opaque or electron-transparent. It contained smaller solid and/or liquid particles inside or on the edge.

3.2. Change of UFP size distribution with distance from I-405

UFP number size distributions were monitored continuously using the SMPS during sample collection. Distributions obtained at the middle of each sampling period are shown for measurements made on I-405 (Fig. 2a) and at distances 30, 60, and 90 downwind of I-405 (Fig. 2b–d, respectively). The geometric mean diameter (μ_g) and geometric standard deviation (σ_g) are shown for distinct modes of the distributions. A small-size mode with μ_g 14.3 ± 1.5 nm was prevalent in the on-freeway distribution. This mode decreased with increasing distance from the freeway, and a larger size mode with μ_g 35.9 ± 2.9 nm became dominant at 90 m. This is similar to what Zhu et al. (2002a) had observed previously, that the concentration of the smaller particles (<25 nm) decreased more dramatically than the larger (25–100 nm) particles with increasing distance from the freeway. These observations suggest

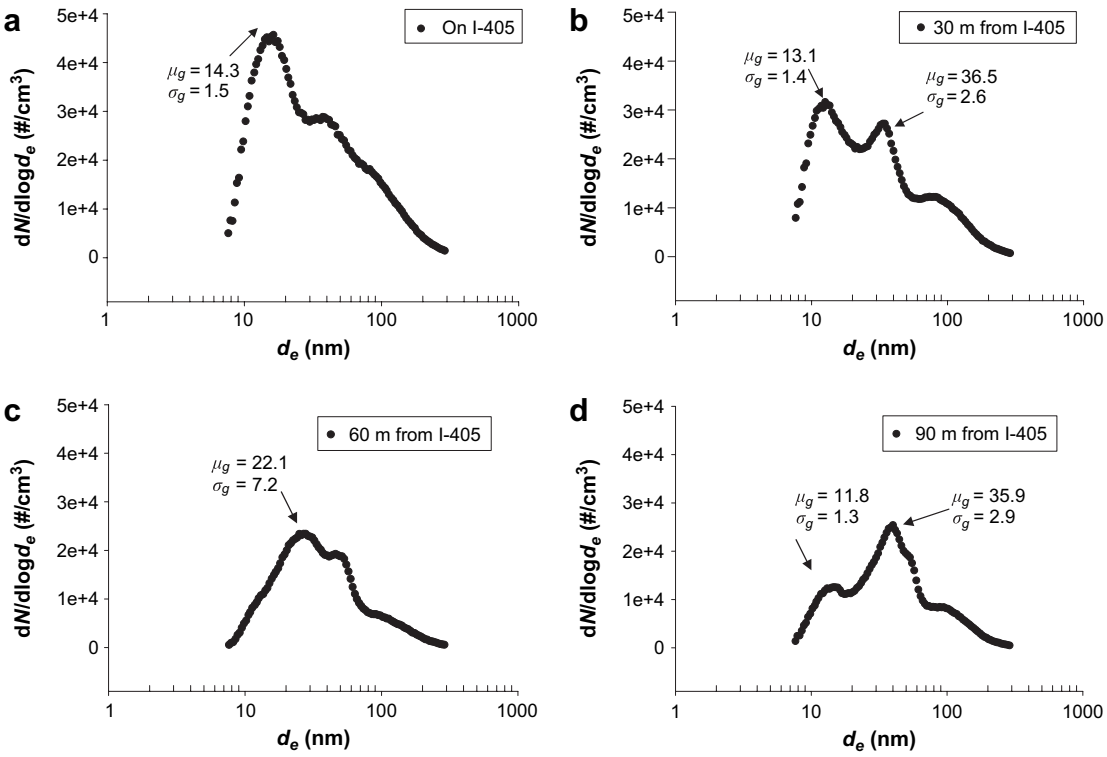

Fig. 2. Aerosol number–size distributions measured (a) on I-405, and (b) 30 m, (c) 60 m, and (d) 90 m downwind from I-405. The geometric mean diameter (μ_g) and geometric standard deviation (σ_g) are shown for distinct modes of the distribution. Measurements were made with a scanning mobility particle sizer (SMPS) on April 21, 2006 for (a), and on April 24, 2006 for (b)–(d).

particles in the smaller modes may coagulate and shift to the larger modes while moving away from the I-405. The data of Zhu et al. (2002a) were simulated later using a multi-component sectional aerosol dynamic model (Zhang et al., 2004). The model included mechanisms of condensation and evaporation. There was good agreement between the predicted and measured number–size distributions, and coagulation was expected to have a minor effect. Subsequently, we analyzed UFP morphology change with distance from the I-405 to provide insight on the processes involved in altering the number–size distribution. Based on our analysis presented in the "NAS UFP Collection Efficiency" section, we compared the fraction of particles in a given morphology class at distances from the freeway.

3.3. Change of UFP morphology with distance from I-405

Individual 50 nm d_e particles collected on- and near-I-405 were grouped according to material contrast in the TEM. Previous studies have indicated that atmospheric and vehicle-emitted UFPs which differ in contrast in the TEM after bombardment with the electron beam may differ in chemical composition and volatility (Okada and Heintzenberg, 2003; Mathis et al., 2004). Because individual particles composed of differently contrasting materials in the TEM may be composed of different substances, we interpret these particles to be internally mixed. The number fraction of electron-opaque, electron-transparent, and internally mixed particles at varying distance downwind of I-405 is presented in Fig. 3. Most (>90%) of the electron-opaque particles were encapsulated by electron-transparent material. The encapsulated particles included aggregates, spheres, and irregularly shaped particles. The term "encapsulated" was initiated by Fuller et al. (1999) and reiterated by Bond and Bergstrom (2006) to describe heterogeneously internally mixed aerosol. Encapsulated is preferred to the often-used "shell and core" term, since "shell and core" implies concentricity, while in fact the immersed particle may be off center. Electron-transparent material which encapsulated one or two electron-opaque particles comprised 38–62% of the total aerosol collected. Multiple (>2) small particles included inside or on the edge of an individual particle (electron-opaque or -transparent) comprised 4–19% of the total. Thus, a large number fraction (57–66%) of particles present in on- and near-freeway samples consisted of heterogeneously internally mixed aerosol. Electron-opaque particles that were not encapsulated were few (1–4%). Electron-transparent spheres comprised a fairly large fraction of the total (29–39%). Thus, most (96–99%) of the 50 nm d_e on- and near-freeway particles were at least partially associated with electron-transparent material. Khun et al. (2005) observed that most (94%) of 40 nm d_e near-freeway particles were associated with volatile material.

The number fraction of particles in given morphology classes at increasing distance downwind of I-405 was compared. The fraction of aggregates was significantly greater on-freeway than 90 m downwind (p-value < 0.01)

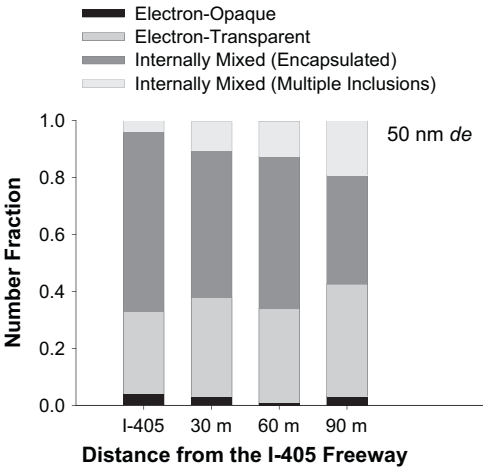

Fig. 3. The number fraction of 50 nm d_e particles on-freeway (I-405) and at increasing distances downwind from the freeway (30, 60 and 90 m) present in given classes of material contrast in the TEM. Individual particles composed of differently contrasting materials are interpreted as internally mixed. The bars from bottom to top represent (1) electron-opaque, (2) electron-transparent, (3) electron-opaque particles encapsulated by electron-transparent material and (4) electron-opaque or -transparent particles which included multiple smaller particles inside or on the edge.

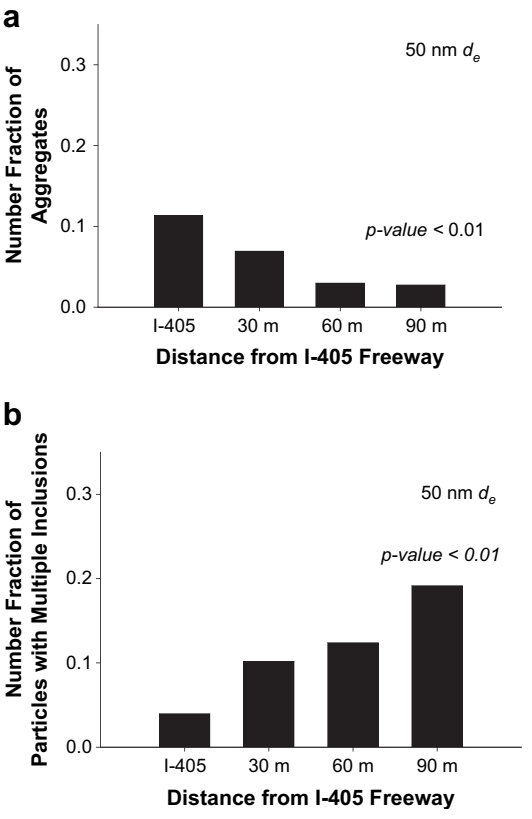

Fig 4. The number fraction of 50 nm d_e particles on-freeway (I-405) and at 30, 60, and 90 m downwind of the freeway that was present as (a) aggregates and (b) particles with multiple inclusions. (a) The fraction of aggregates decreased with increasing distance from the freeway. The fraction at 90 m was significantly less ($p = 0.001$) than the fraction on-freeway. (b) The fraction of particles with multiple inclusions increased with increasing distance from the freeway. The fraction at 90 m was significantly greater ($p < 0.001$) than the fraction on-freeway.

(Fig. 4a). Since aggregates are a primary aerosol (directly emitted), this may indicate that secondary aerosol (formed in the atmosphere) becomes more prominent with increasing distance from the freeway. The result is consistent with the findings of Dye et al. (2000), who measured larger fractions of aggregates near the roadway than in urban background aerosol in Plymouth, UK. The fraction of total aerosol present as particles with multiple inclusions was significantly less on-freeway than 90 m downwind (p-value < 0.01) (Fig. 4b). The increase in particles with multiple inclusions with increasing distance from the freeway suggests that dilution does not prevent particles from colliding and merging. Thus, coagulation may play a role in altering the number–size distribution and deserve further investigation near roadways.

The above results on the change in morphology with increasing distance from I-405 pertain to UFPs with a narrow range of 50 ± 3 nm d_e. The total aerosol near I-405 was also sampled by the NAS to observe whether the same trends are present over a wider diameter range. Because the NAS collection efficiency depends on the particle diameter, all particle sizes are not collected in the same proportion. Particles smaller than 80 nm d_e are collected with greater than 50% efficiency; and those larger than 80 nm d_e with less than 50% efficiency. Thus, the fraction of particles in each size range in the samples is not equal to the fraction present in the atmosphere. However, the total aerosol samples collected by the NAS (which largely consist of particles with diameters less than 80 nm d_e as shown in Fig. 2) were analyzed to determine whether changes in morphology were consistent with those for 50 nm d_e particles. These results are shown in Fig. 5. The fraction of aggregates on-freeway was much greater than the fraction at 30 m from the freeway (Fig. 5a). This is consistent with the results for 50 nm d_e particles and the trend is more pronounced. The fraction of particles with multiple inclusions on-freeway is less than the fraction at 30 m (Fig. 5b). The increase in particles with multiple inclusions with increasing distance from the freeway is in agreement with the results for 50 nm d_e particles. Thus, the change in the fraction of aggregates and particles with multiple inclusions for near-freeway aerosol which largely consists of particles with diameters less than 80 nm is similar to that for 50 nm d_e particles.

3.4. Morphology comparison between I-405 and I-710 freeways

The fraction of 50 nm d_e particles in individual morphology classes collected on I-405 was compared to those collected on I-710 and is shown in Fig. 6. Heavy-duty diesel traffic is greater on I-710 than I-405 (Zhu et al., 2002b). Diesel engines emit higher number concentrations of particulate matter (Kittelson, 1998) and larger masses of elemental carbon (Kittelson et al., 2001) than spark-ignition engines. Diesel exhaust particles which consist of elemental carbon are probably present as aggregates (Kittelson, 1998; Clauge et al., 1999; Park et al., 2004b). However, higher

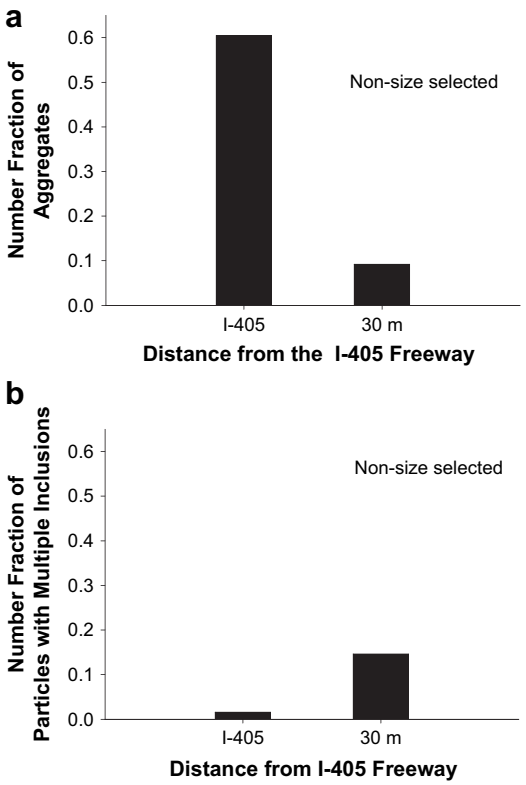

Fig. 5. The number fraction of non-size selected particles that were present as (a) aggregates and (b) particles with multiple inclusions on-freeway (I-405) and at 30 m downwind of the freeway. Similar to the results for 50 nm d_e particles, (a) the fraction of aggregates decreased and (b) the fraction of particles with multiple inclusions increased 30 m from the freeway.

fractions of aggregates were present on I-405, which is mostly traveled by gasoline powered vehicles. The result is consistent with a recent single particle mass spectral study which showed that elemental carbon particles dominated gasoline emitted UFP number concentrations (Sodeman et al., 2005). In addition, the most abundant diesel exhaust particles may have larger diameters than spark-ignition exhaust particles (Maricq et al., 1999; Morawska et al., 1998; Holmes et al., 2005). Thus, diesel exhaust may contribute fewer 50 nm d_e aggregates than spark-ignition exhaust. A higher fraction of particles with multiple inclusions was present on I-710 than I-405. This may be due to differences in meteorological conditions and traffic density. During sampling on I-710, the wind was weaker than during the I-405 sampling; wind speeds were 2.6 mph on I-710 and 6.6 mph on I-405. In addition, UFPs were more abundant on I-710 (8.55×10^4 # cm^{-3}) than I-405 (4.88×10^4 # cm^{-3}). Vehicle-emitted particles may have experienced less dilution and a greater residence time in a concentrated plume for coagulation to occur. Additional studies in varying meteorological conditions and traffic densities are needed to test the above explanation. Similar to I-405, most electron-opaque particles (aggregates, spheres, and irregularly shaped) on I-710 were encapsulated by electron-transparent material. This suggests that a large fraction of 50 nm d_e particles on I-710 was heterogeneously internally mixed. In addition, most (>90%) 50 nm d_e particles collected on I-710 were at least partially associated with electron-transparent material, consistent with observations on I-405.

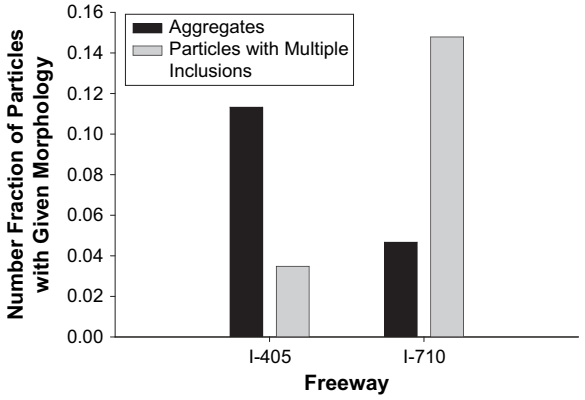

Fig. 6. The number fraction of 50 nm d_e particles in given morphology classes on I-405 and I-710. The fraction of aggregates (black bar) on I-405 was greater than that on I-710. The fraction of particles with multiple inclusions (grey bar) was greater on I-710 than I-405.

4. Conclusions

The spatial variation of atmospheric UFP morphology was investigated near a major Los Angeles freeway by selecting particles with a narrow range of electrical mobility diameters with a DMA and collecting samples for TEM analysis using the NAS. Calculations based on theory suggest an aggregate and a sphere would not be differentially collected by diffusion and thus, their disproportionate collection may not result. In addition, from estimates of the Stokes number, inertial impaction is not expected to contribute significantly to the collection of particles with spherical and aggregate morphology. However, because these predictions have not been tested experimentally, we do not compare fractions of particles in different morphology classes. Instead, we compare the fraction of particles in a given morphology class at distances from the freeway.

The change in the fraction of particles present in a given morphology class with distance from I-405 was investigated to gain insight on the aerosol mechanisms involved in altering the number–size distribution. For samples collected on- and near-I-405, most electron-opaque particles (aggregates, spheres, irregularly shaped) were encapsulated by an electron-transparent material. This may provide evidence that the 50 nm d_e near-freeway aerosol was largely internally mixed. Measurements of individual particle chemical composition would be valuable for evaluating mixing properties in a future study. The fraction of aggregates measured on I-405 was significantly greater than the fraction at 90 m (p-value < 0.01). Aggregates are a primary aerosol and their relative decrease may indicate that secondary aerosol becomes more abundant downwind of the freeway. The fraction of particles with multiple inclusions measured on I-405 was significantly less than the fraction at 90 m (p-value < 0.01). Despite dilution of the

exhaust plume downwind of the freeway, particles may collide and merge causing an increase in the fraction of particles with multiple inclusions. Thus, coagulation may play a role in altering the particle size distribution. Future studies are needed which compare the spatial variation of near-freeway UFP morphology at varying meteorological conditions and traffic densities.

Acknowledgements

The authors thank Nancy Jennerjohn for help with field sampling, and Prof. Sheldon K. Friedlander and Dr. Anshuman A. Lall for their discussions on aggregate electrical mobility diameter. This work was supported by the Southern California Particle Center and Supersite: U.S. Environmental Protection Agency grant number R82735201, California Air Resources Board contract number 04-324 and the Southern California Environmental Health Center, National Institute of Environmental Health Sciences (NIEHS) Grant # 5 P30 ES07048.

References

Barone, T.L., Lall, A.A., Zhu, Y., Yu, R.C., Friedlander, S.K., 2006. Inertial deposition of nanoparticle chain aggregates: theory and comparison with impactor data for ultrafine atmospheric aerosols. Journal of Nanoparticle Research 8, 669–680.

Bérubé, K.A., Jones, T.P., Williamson, B.J., Winters, C., Morgan, A.J., Richards, R.J., 1999. Physicochemical characterization of diesel exhaust particles: factors for assessing biological activity. Atmospheric Environment 33, 1599–1614.

Bond, T.C., Bergstrom, R.W., 2006. Light absorption by carbonaceous particles: an investigative review. Aerosol Science and Technology 40, 27–67.

Cass, G.R., Hughes, L.S., Bhave, P., Kleeman, M.J., Allen, J.O., Salmon, L.G., 2000. The chemical composition of atmospheric ultrafine particles. Philosophical Transactions of the Royal Society of London A 358, 2581–2592.

Chakrabarty, R.K., Moosmuller, H., Arnott, W.P., Garro, M.A., Walker, J.W., 2006. Structural and fractal properties of particles emitted from spark ignition engines. Environmental Science and Technology 40, 6647–6654.

Chan, P., Dahneke, B., 1981. Free-molecule drag on straight chains of uniform spheres. Journal of Applied Physics 52, 3106–3110.

Chen, Y., Shah, N., Huggins, F.E., Huffman, G.P., 2004. Investigations of microcharacteristics of PM2.5 in residual oil fly ash by analytical transmission electron microscopy. Environmental Science and Technology 38, 6553–6560.

Clauge, A.D.H., Donnet, J.B., Wang, T.K., Peng, J.C.M., 1999. A comparison of diesel engine soot with carbon black. Carbon 37, 1553–1565.

Dahneke, B., 1982. Viscous resistance of straight-chain aggregates of uniform spheres. Aerosol Science and Technology 1, 179–185.

Dixkens, J., Fissan, H., 1999. Development of an electrostatic precipitator for off-line particle analysis. Aerosol Science and Technology 30, 438–453.

Dye, A.L., Rhead, M.M., Trier, C.J., 2000. The quantitative morphology of roadside and background urban aerosol in Plymouth, UK. Atmospheric Environment 34, 3139–3148.

Friedlander, S.K., 2000. Smoke, Dusk, and Haze: Fundamentals of Aerosol Dynamics, second ed. Oxford University Press, Oxford, pp. 32–40.

Fuller, K.A., Malm, W.C., Kreidenweis, S.M., 1999. Effects of mixing on extinction by carbonaceous particles. Journal of Geophysical Research 104, 15941–15945.

Hinds, W.C., 1999. Aerosol Technology: Properties, Behavior, and Measurement of Airborne Particles, second ed. Wiley, New York, p. 121.

Holmes, N.S., Morawska, L., Mengersen, K., Jayaratne, E.R., 2005. Spatial distribution of submicrometre particles and CO in an urban microscale environment. Atmospheric Environment 39, 3977–3988.

Kasper, G., Shaw, D.T., 1983. Comparative size distribution measurements on chain aggregates. Aerosol Science and Technology 2, 369–381.

Katrinak, K.A., Rez, P., Perkes, P.R., Buseck, P.R., 1993. Fractal geometry of carbonaceous aggregates from an urban aerosol. Environmental Science and Technology 27, 539–547.

Khun, T., Biswas, S., Fine, P.M., Geller, M., Sioutas, C., 2005. Physical and chemical characteristics and volatility of PM in the proximity of a light-duty vehicle freeway. Aerosol Science and Technology 39, 347–357.

Kim, S., Jaques, P.A., Chang, M.C., Froines, J.R., Sioutas, C., 2001. Versatile aerosol concentration enrichment system (VACES) for simultaneous in vivo and in vitro evaluation of toxic effects of ultrafine, fine and coarse ambient particles. 1. Development and laboratory characterization. Journal of Aerosol Science 32, 1281–1297.

Kittelson, D.B., 1998. Engines and nanoparticles: a review. Journal of Aerosol Science 29, 575–588.

Kittelson, D.B., Watts, W.F., Johnson, J.P., 2001. Fine particle (nanoparticle) emissions on Minnesota highways, Minnesota Department of Transportation.

Lall, A.A., Friedlander, S.K., 2006. On-line measurement of ultrafine aggregate surface area and volume distributions by electrical mobility analysis. 1. Theoretical analysis. Journal of Aerosol Science 37, 260–271.

Maricq, M.M., Podsiadlik, D.H., Chase, R.E., 1999. Examination of the size-resolved and transient nature of motor vehicle particle emissions. Environmental Science and Technology 33, 1618–1626.

Mathis, U., Kaegi, R., Mohr, M., Zenobi, R., 2004. TEM analysis of volatile nanoparticles from particle trap equipped diesel and direct-injection spark-ignition vehicles. Atmospheric Environment 38, 4347–4355.

Morawska, L., Thomas, S., Bofinger, N., Wainwright, D., Neale, D., 1998. Comprehensive characterization of aerosols in a subtropical urban atmosphere: particle size distribution and correlation with gaseous pollutants. Atmospheric Environment 32, 2467–2478.

Morigi, M.P., Giacomelli, G.M., Prodi, V., 1999. Mineral fiber sampling and size selection. Annals of Occupational Hygiene 43, 117–124.

Okada, K., Heintzenberg, J., 2003. Size distribution, state of mixture, and morphology of urban aerosol particles at given electrical mobilities. Journal of Aerosol Science 34, 1539–1553.

Oberdörster, G., 2001. Pulmonary effects of inhaled ultrafine particles. Occupational and Environmental Health 74, 1–8.

Park, K., Kittelson, D.B., Zachariah, M.R., McMurry, P.H., 2004a. Measurement of inherent material density of nanoparticle agglomerates. Journal of Nanoparticle Research 6, 267–272.

Park, K., Kittelson, D.B., McMurry, P.H., 2004b. Structural properties of diesel exhaust particles measured by transmission electron microscopy (TEM): relationships to particle mass and mobility. Aerosol Science and Technology 38, 881–889.

Rönkkö, T., Virtanen, A., Kannosto, J., Keskinen, J., Lappi, M., Pirjola, L., 2007. Nucleation mode particles with a nonvolatile core in the exhaust of a heavy-duty diesel vehicle. Environmental Science and Technology 41, 6384–6389.

Shi, Z., Shao, L., Jones, T.P., Whittaker, A.G., Lu, S., Bérubé, K.A., He, T., Richards, R.J., 2003. Characterization of airborne individual particles collected in an urban area, a satellite city and a clean air area in Beijing, 2001. Atmospheric Environment 37, 4097–4108.

Sodeman, D.A., Toner, S.M., Prather, K.A., 2005. Determination of single particle mass spectral signatures from light-duty vehicle emissions. Environmental Science and Technology 39, 4569–4580.

Stearns, R.C., Paulauskis, J.D., Godleski, J.J., 2001. Endocytosis of ultrafine particles by A549 cells. American Journal of Respiratory Cell and Molecular Biology 24, 108–115.

Inc., T.S.I., 2001. Model 3089 Nanometer Aerosol Sampler Instruction Manual. TSI Inc., St. Paul, MN.

Wentzel, M., Gorzawski, H., Naumann, K.H., Saathoff, H., Weinbruch, S., 2003. Transmission electron microscopical and aerosol dynamical characterization of soot aerosols. Journal of Aerosol Science 34, 1347–1370.

Xiong, C., Friedlander, S.K., 2001. Morphological properties of atmospheric aerosol aggregates. Proceedings of the National Academy of Sciences of the United States of America 98, 11851–11856.

Yue, W., Li, X., Liu, J., Li, Y., Yu, X., Deng, B., Wan, T., Zhang, G., Hunag, Y., He, W., Hua, W., Shao, L., Li, W., Yang, S., 2006. Characterization of PM2.5 in the ambient air of Shanghai city by analyzing individual particles. Science of the Total Environment 368, 916–925.

Zhang, K.M., Wexler, A.S., Zhu, Y.F., Hinds, W.C., Sioutas, C., 2004. Evolution of particle number distribution near roadways. Part II: the

'Road-to-Ambient' process. Atmospheric Environment 38, 6655–6665.

Zhu, Y., Hinds, W.C., Kim, S., Sioutas, C., 2002a. Concentration and size distribution of ultrafine particles near a major highway. Journal of Air and Waste Management Association 52, 174–185.

Zhu, Y.F., Hinds, W.C., Kim, S., Shen, S., Sioutas, C., 2002b. Study of ultrafine particles near a major highway with heavy-duty diesel traffic. Atmospheric Environment 36, 4323–4335.

Zhu, Y., Hinds, W.C., Shen, S., Sioutas, C., 2004. Seasonal trends of concentration and size distribution of ultrafine particles near major highways in Los Angeles. Aerosol Science and Technology 38, 5–13.

Zhu, Y.F., Fung, D., Kennedy, N., Hinds, W.C., Eiguren-Fernandez, A., 2008. Measurements of ultrafine particles and other vehicular pollutants inside a mobile exposure system on Los Angeles freeways. Journal of Air and Waste Management Association 58, 424–434.